Applied Physics Letters

Depth resolved luminescence from oriented ZnO nanowires

R. A. Rosenberg, M. Abu Haija, K. Vijayalakshmi, J. Zhou, S. Xu et al.

Citation: Appl. Phys. Lett. 95, 243101 (2009); doi: 10.1063/1.3275000
View online: http://dx.doi.org/10.1063/1.3275000
View Table of Contents: http://apl.aip.org/resource/1/APPLAB/v95/i24
Published by the AIP Publishing LLC.

Additional information on Appl. Phys. Lett.

Journal Homepage: http://apl.aip.org/
Journal Information: http://apl.aip.org/about/about_the_journal
Top downloads: http://apl.aip.org/features/most_downloaded
Information for Authors: http://apl.aip.org/authors

Downloaded 09 Oct 2013 to 130.126.32.13. This article is copyrighted as indicated in the abstract. Reuse of AIP content is subject to the terms at: http://apl.aip.org/about/rights_and_permissions

Depth resolved luminescence from oriented ZnO nanowires

R. A. Rosenberg,[1,a)] M. Abu Haija,[1] K. Vijayalakshmi,[1] J. Zhou,[2] S. Xu,[2] and Z. L. Wang[2]
[1]*Advanced Photon Source, Argonne National Laboratory, Argonne, Illinois 60439, USA*
[2]*School of Material Science and Engineering, Georgia Institute of Technology, Atlanta, Georgia 30332, USA*

(Received 6 October 2009; accepted 21 November 2009; published online 14 December 2009)

We have utilized the limited penetration depth of x-rays to study the near-surface properties of vertically aligned ZnO nanowires. For an energy of 600 eV the penetration depth varies between 3 and 132 nm as the incidence angle changes from 2° to 33°. Thus, by obtaining optical luminescence spectra as a function of incidence angle, it is possible to probe the near-surface region with nanometer-scale resolution. We will present angle dependent optical luminescence data from oriented ZnO nanowires. By fitting the results to a simple model, we extract a depth for the surface defect regions of ~14 nm. © *2009 American Institute of Physics*. [doi:10.1063/1.3275000]

Nanodevices based on wide band gap semiconductors have great potential in applications running from photon detectors to gas sensors. Critical to their successful implementation is knowledge of the surface and interfacial properties. One of the most promising candidates for such applications is ZnO-based structures. ZnO thin films have found a wide range of applications including catalysis, varistors, surface acoustic wave devices, sensors, and transducers.[1] Its wurtzite structure leads to strong pyroelectric and piezoelectric properties. Due to its wide band gap (3.37 eV) and high exciton binding energy (60 meV), ZnO has potential for a wide range of optoelectronic applications. In recent years a plethora of ZnO nanostructures has been produced, which has led to a wide range of studies into their electrical, chemical, and mechanical properties.[2] The discovery of room-temperature UV lasing[3] in ZnO nanowires has stimulated a considerable effort into understanding its optical properties.

The luminescent properties of bulk and nanostructured ZnO have been reviewed recently.[4,5] The band gap emission consists of excitonic and donor acceptor pair transitions along with their phonon replicas. Analogous luminescence is seen in nanostructures as well. At lower energies (1.7–2.7 eV) emission from defect states is often observed. The relative intensity and energy position of defect state emission varies from sample to sample.[4,6–9] The exact assignment of the transitions is controversial. The general consensus for the green, 2.4 eV emission is that it stems from oxygen vacancies near the surface. At lower energies, ~2 eV, orange luminescence is often observed and has been assigned to interstitial oxygen ions.[4,6]

X-ray excited optical luminescence (XEOL) has been shown to be a powerful tool for investigating the local chemical environment of a site that gives rise to a particular luminescent band.[10] Recently, we have used XEOL to understand the nature of the band gap and defect luminescence from ZnO nanowires[11] and identify the origin of the luminescence from ZnO-MgZnO nanoheterostructures.[12] In the present work, we have utilized the limited penetration depth of soft x-rays to study the near-surface properties of vertically aligned ZnO nanowires. For an x-ray energy of 600 eV the penetration depth varies between 3 and 132 nm as the incidence angle changes from 2° to 33°. Thus, by obtaining optical luminescence spectra as a function of angle it is possible to probe the near surface region with nanometer-scale resolution. We will present angle dependent optical luminescence data from oriented ZnO nanowires. By fitting the results to a simple model we extract a depth for the surface defect region of ~14 nm, which is in line with the conclusions from previous photoluminescence and cathodoluminescence studies.[13–17]

The ZnO nanowires were prepared on gold coated Si substrates by the hydrothermal decomposition method which has been described previously.[18,19] The experiments were performed using soft x-rays from beamline 4-ID-C at the Advanced Photon Source. This facility provides intense, tunable radiation in the range 500–3000 eV. The x-rays irradiated the sample at varying angles, α, with respect to the substrate normal, which coincides with the *c*-axis of the nominally perpendicularly aligned nanowires. The emitted optical photons were extracted at 45° with respect to the x-ray beam using a condenser lens and then focused on the entrance slit of a 0.3 m monochromator. A cooled photomultiplier tube was used to detect the dispersed photons. The sample was mounted on a manipulator located in an ultrahigh-vacuum end station. All data presented here were obtained at an x-ray energy of 600 eV and a sample temperature of ~35 K.

XEOL spectra of two different nanowire samples obtained at a relatively large angle (α=33°) are shown in Fig. 1. In Fig. 1(a) are the data from sample A (~720 nm diameter and 3.87 μm length) and results from sample E (~390 nm diameter and 3.29 μm length) are shown in Fig. 1(b). The insets are scanning electron microscopy (SEM) images of the two samples. Both spectra show a sharp, band gap exciton (BGE) peak at ~3.36 eV and a broad, defect-related peak at ~2 eV. The sharp feature at ~1.7 eV is due to the BGE peak dispersed in second order.

The intensities of the various peaks are obtained by least-squares curve fitting the spectra to Gaussian components. The BGE peak is composed of free and bound excitons as well as their phonon replicas.[5] To simulate this complex shape, a sum of four components located at 3.34, 3.30, 3.26, and 3.19 eV of varying widths was employed. For the

a)Electronic mail: rosenberg@aps.anl.gov.

 © 2009 American Institute of Physics

Downloaded 09 Oct 2013 to 130.126.32.13. This article is copyrighted as indicated in the abstract. Reuse of AIP content is subject to the terms at: http://apl.aip.org/about/rights_and_permissions

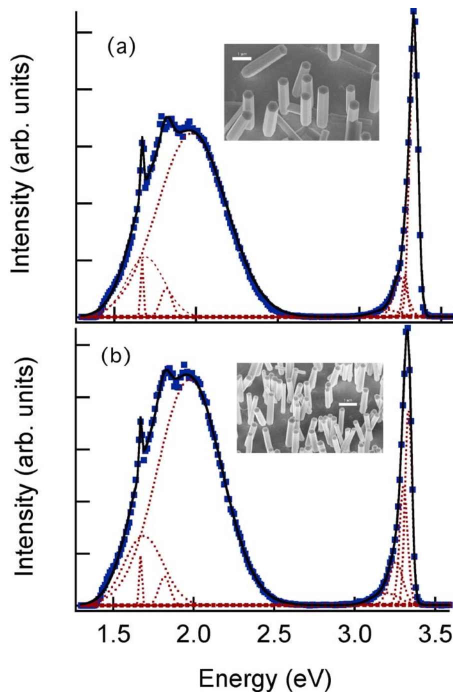

FIG. 1. (Color online) Luminescence spectra of ZnO nanowire samples A (a) and E (b) obtained with 600 eV x-rays and a grazing angle of 33°. Also shown are the results of curve fitting to Gaussian components. The dotted (red) lines are the individual components and the solid (black) line is the simulated curve. The insets show SEM images of the two samples. The white scale bar represents 1 μm.

broad defect level peak the minimum number of components that were necessary for a reasonable fit were three, located at 1.97, 1.82, and 1.70 eV. The 1.97 eV peak was by far the most intense defect component in all the spectra. In addition, a component located at 1.67 eV was employed to simulate the second-order BGE peak. Some results of the fitting procedure are seen in Figs. 1 and 2.

To gain insight into the depth variation in the sites responsible for the luminescence peaks, XEOL spectra were obtained as a function of the angle α between the x-ray propagation vector and the c-axis of the nanowire. Results for sample E are shown in Fig. 2. For all the spectra the peak

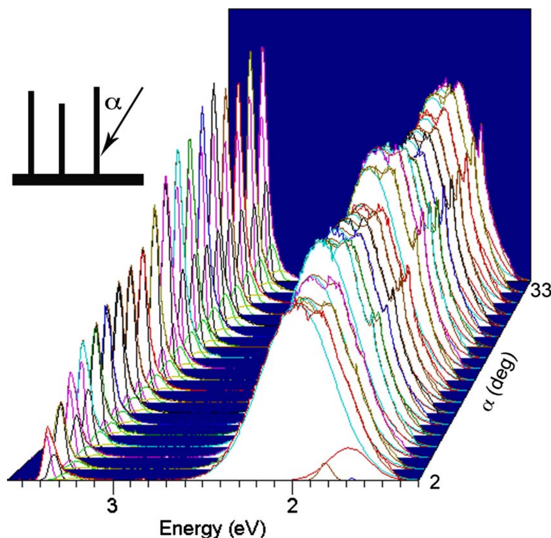

FIG. 2. (Color online) Angle-dependent luminescence data from sample E at an x-ray energy of 600 eV.

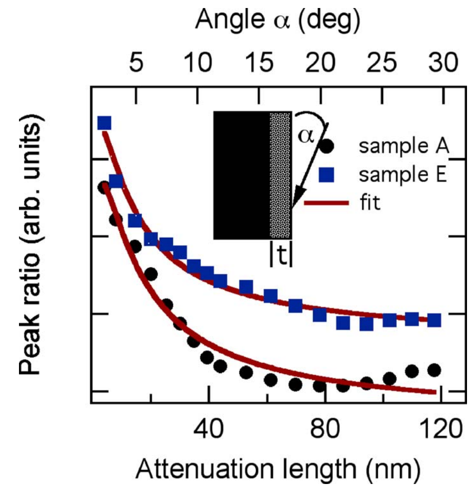

FIG. 3. (Color online) The points show the ratio of the 1.97 eV component to the sum of the band-gap exciton components for sample A (circles) and sample E (squares) as a function of x-ray penetration depth (bottom axis) or incident angle (top axis). The solid line is the simulated curve from fitting the data to Eq. (3).

positions and widths were fixed; only the intensities were allowed to vary. As α increases, the overall intensity increases and the ratio (R) of the defect to BGE luminescence peaks decreases. The overall increase in intensity is due to a higher collection efficiency of the luminescence as the sample is rotated toward the collection optics. R decreases as a result of the increase in x-ray penetration depth with increasing incident angle.[20] As the x-rays probe deeper they sample less of the surface region, which is responsible for the defect luminescence.

To analyze these data we utilized the model developed by Emura *et al.*[21] The XEOL yield as a function of x-ray penetration depth, x, is given by

$$dN(x) = \mu \eta I_0 \exp(-\mu x)dx, \quad (1)$$

where μ is the x-ray absorption coefficient, η is the total yield of optical luminescence, and I_0 is the incident x-ray intensity. If the assumption is made that the defect luminescence is confined to a thin surface layer of thickness t, then after integration the following equation can be derived:

$$N = \eta I_0[1 - \exp(-\mu t)]. \quad (2)$$

Thus, by fitting the angle (penetration depth)-dependent luminescence intensity data to a function of the form:

$$N = K[1 - \exp(-t/d)] + B, \quad (3)$$

where d is the penetration depth and B is a background level, it should be possible to extract the thickness t. However, it is not possible to directly apply Eq. (3) to the absolute intensities. As already mentioned the collection efficiency of the optics changes as a function of angle. In addition, the nanowires are shadowed by both their ends and each other in an unknown manner. Therefore we make the assumption that the BGE peak intensity is uniform throughout the nanowire,[16] and examine the ratio, R, as a function of angle/x-ray penetration depth.[20]

In Fig. 3 the data points show the ratio of the 1.97 eV peak to the sum of the four components of the BGE peak as a function of angle (top axis) or the corresponding penetration depth[20] (bottom axis). Similar results were obtained for

Downloaded 09 Oct 2013 to 130.126.32.13. This article is copyrighted as indicated in the abstract. Reuse of AIP content is subject to the terms at: http://apl.aip.org/about/rights_and_permissions

the 1.82 and 1.70 eV components. The solid lines are the results of a fit of Eq. (3) to the data points. Although there is some deviation of the data from the fitted curve, particularly for sample A, the agreement is reasonable considering the simplicity of the model. In addition, while the nanowires are nominally aligned normal to the substrate, there is considerable variation of the nanowire orientation (see Fig. 1). The extracted defect level thicknesses are 15 ± 3 and 14 ± 2 nm for samples A and E, respectively. These values should be regarded as upper limits to the thickness. The model was derived for a geometry in which the sample surface, sample normal, and x-ray propagation vector were all in the same plane. This would only be the case for perfectly aligned, rectangular nanowires. Since the ZnO nanowires are hexagonal with random azimuthal orientations, there will be many instances where the x-rays are incident at a more oblique angle with respect to the sample surface/normal plane. This will result in a larger effective defect layer thickness. In addition migration of electron-hole pairs within a certain radius can also contribute to the luminescence. For ZnO this radius can be estimated[10] to be ~ 8 nm and will contribute to the uncertainty of the derived thicknesses.

A major assumption used in deriving this model was that the BGE luminescence was uniform throughout the region probed by the x-rays. Although this premise has been used in previous studies, we thought it is worthwhile to try to check it, since it is well known that surface defects often quench BGE emission. In order to do this we developed models in which there was a "dead" layer for the BGE luminescence or where the BGE emission was exponentially attenuated near the surface. In both cases the fit of the model to the data was significantly worse.

Previous work has also investigated the depth dependence of defect luminescence in ZnO nanostructures. In a study by Shalish *et al.*,[15] the intensity of the 2.4 eV defect peak was shown to be inversely proportional to the size of the nanowire, which indicates that it is due to defects (singly ionized oxygen vacancies near the surface [~ 30 nm]).[22] However, a number of other papers have suggested other possible assignments.[7,23] Cathodoluminescence studies of the 2.4 eV emission indicate that it is localized within a 10 nm region near the surface.[14,16]

To our knowledge there have been no previous depth-dependent studies on ZnO nanostructures of the orange, ~ 2 eV emission seen in the present work. Ong and Du have presented cathodoluminescence studies of a 2.05 eV emission from ZnO films which indicate it arises from the bulk, although a 1.78 eV peak seems to be localized near the surface.[24] Other groups have also reported orange luminescence from nanostructures,[4,6,25] thin films,[26,27] and crystals.[28] In the present work the 1.97 eV component, as well as the 1.82 and 1.70 eV components appear to originate from a near-surface region of 10–15 nm in width. If they are associated with oxygen interstitial defects then they must be localized within this region, which is at odds with conclusions drawn from some of the previous work.

Depth-dependent XEOL measurements have great potential for understanding defect distributions and in the future we plan to investigate oriented ZnO nanostructures grown under varying conditions as well as other aligned nanomaterials. Correlating such results with information obtained by complementary x-ray absorption and photoemission techniques will enable researchers to get a more thorough grasp of the surface and interfacial electronic structure of any aligned nanostructure.

This work was performed at the Advanced Photon Source and was supported by the U.S. Department of Energy, Office of Science, Office of Basic Energy Sciences under Contract No. DE-AC02-06CH11357.

[1] S. J. Pearton, D. P. Norton, K. Ip, Y. W. Heo, and T. Steiner, J. Vac. Sci. Technol. B **22**, 932 (2004).
[2] Z. L. Wang, J. Phys.: Condens. Matter **16**, R829 (2004).
[3] M. H. Huang, S. Mao, H. Feick, H. Yan, Y. Wu, H. Kind, E. Weber, R. Russo, and P. Yang, Science **292**, 1897 (2001).
[4] A. B. Djurišić and Y. H. Leung, Small **2**, 944 (2006).
[5] Ü. Özgür, Y. I. Alivov, C. Liu, A. Teke, M. A. Reshchikov, S. Dogan, V. Avrutin, S. J. Cho, and H. Morkoc, J. Appl. Phys. **98**, 041301 (2005).
[6] L. E. Greene, M. Law, J. Goldberger, F. Kim, J. C. Johnson, Y. Zhang, R. J. Saykally, and P. Yang, Angew. Chem., Int. Ed. **42**, 3031 (2003).
[7] D. Li, Y. H. Leung, A. B. Djurišić, Z. T. Liu, M. H. Xie, S. L. Shi, S. J. Xu, and W. K. Chan, Appl. Phys. Lett. **85**, 1601 (2004).
[8] M. A. Reshchikov, H. MorkoÁ, B. Nemeth, J. Nause, J. Xie, B. Hertog, and A. Osinsky, Physica B **401**, 358 (2007).
[9] K. H. Tam, C. K. Cheung, Y. H. Leung, A. B. Djurišić, C. C. Ling, C. D. Beling, S. Fung, W. M. Kwok, W. K. Chan, D. L. Phillips, L. Ding, and W. K. Ge, J. Phys. Chem. B **110**, 20865 (2006).
[10] A. Rogalev and J. Goulon, in *Chemical Applications of Synchrotron Radiation, Part II: X-ray Applications*, edited by T. K. Sham (World Scientific, Singapore, 2002), Vol. 12B, p. 707.
[11] R. A. Rosenberg, G. K. Shenoy, L. C. Tien, D. Norton, S. Pearton, X. H. Sun, and T. K. Sham, Appl. Phys. Lett. **89**, 093118 (2006).
[12] R. A. Rosenberg, G. K. Shenoy, M. F. Chisholm, L.-C. Tien, D. Norton, and S. Pearton, Nano Lett. **7**, 1521 (2007).
[13] M. Foley, C. Ton-That, and M. R. Phillips, Appl. Phys. Lett. **93**, 243104 (2008).
[14] N. Pan, X. Wang, M. Li, F. Li, and J. G. Hou, J. Phys. Chem. C **111**, 17265 (2007).
[15] I. Shalish, H. Temkin, and V. Narayanamurti, Phys. Rev. B **69**, 245401 (2004).
[16] H. Xue, N. Pan, R. Zeng, M. Li, X. Sun, Z. Ding, X. Wang, and J. G. Hou, J. Phys. Chem. C **113**, 12715 (2009).
[17] J. D. Ye, H. Zhao, W. Liu, S. L. Gu, R. Zhang, Y. D. Zheng, S. T. Tan, X. W. Sun, G. Q. Lo, and K. L. Teo, Appl. Phys. Lett. **92**, 131914 (2008).
[18] S. Xu, C. S. Lao, B. Weintraub, and Z. L. Wang, J. Mater. Res. **23**, 2072 (2008).
[19] S. Xu, Y. Wei, M. Kirkham, J. Liu, W. Mai, D. Davidovic, R. L. Snyder, and Z. L. Wang, J. Am. Chem. Soc. **130**, 14958 (2008).
[20] B. L. Henke, E. Gullikson, and C. Davis, At. Data Nucl. Data Tables **54**, 181 (1993).
[21] S. Emura, T. Moriga, J. Takizawa, M. Nomura, K. R. Bauchspiess, T. Murata, K. Harada, and H. Maeda, Phys. Rev. B **47**, 6918 (1993).
[22] K. Vanheusden, W. L. Warren, C. H. Seager, D. R. Tallant, J. A. Voigt, and B. E. Gnade, J. Appl. Phys. **79**, 7983 (1996).
[23] V. A. L. Roy, A. B. Djurišić, W. K. Chan, J. Gao, H. F. Lui, and C. Surya, Appl. Phys. Lett. **83**, 141 (2003).
[24] H. C. Ong and G. T. Du, J. Cryst. Growth **265**, 471 (2004).
[25] N. Wang, H. Lin, J. Li, L. Zhang, X. Li, J. Wu, and C. Lin, J. Am. Ceram. Soc. **90**, 635 (2007).
[26] S. A. Studenikin, G. Nickolay, and C. Michael, J. Appl. Phys. **84**, 2287 (1998).
[27] X. L. Wu, G. G. Siu, C. L. Fu, and H. C. Ong, Appl. Phys. Lett. **78**, 2285 (2001).
[28] T. Sekiguchi, S. Miyashita, K. Obara, T. Shishido, and N. Sakagami, J. Cryst. Growth **214**, 72 (2000).

Downloaded 09 Oct 2013 to 130.126.32.13. This article is copyrighted as indicated in the abstract. Reuse of AIP content is subject to the terms at: http://apl.aip.org/about/rights_and_permissions